Strål
säkerhets
myndigheten
Swedish Radiation Safety Authority

Research

Modelling Environmental Sensitization of Chromia Forming Nickel Base Alloys Toward Stress Corrosion Cracking in Light Water Reactors by Atomistic Simulations

2024:18

Author: Ageo Meier de Andrade, Christine Geers and Itai Panas
Department of Chemistry and Chemical Engineering, Chalmers
University of Technology, Gothenburg
Jiaxin Chen
Department of Chemistry and Chemical Engineering,
Chalmers University of Technology, Gothenburg
Studsvik Nuclear AB, Nyköping

Date: December 2024
Report number: 2024:18
ISSN: 2000-0456
Available at www.ssm.se

Strål
säkerhets
myndigheten
Swedish Radiation Safety Authority

Author: **Ageo Meier de Andrade, Christine Geers and Itai Panas**
Department of Chemistry and Chemical Engineering, Chalmers
University of Technology, Gothenburg

Jiaxin Chen
Department of Chemistry and Chemical Engineering, Chalmers
University of Technology, Gothenburg

Studsvik Nuclear AB, Nyköping

2024:18

Modelling Environmental Sensitization of Chromia Forming Nickel Base Alloys Toward Stress Corrosion Cracking in Light Water Reactors by Atomistic Simulations

Date: December 2024
Report number: 2024:18
ISSN: 2000-0456
Available at www.stralsakerhetsmyndigheten.se

SSM 2024:18

SSM perspektiv

Bakgrund

Spänningskorrosion (SCC) i lastbärande konstruktioner har varit en långvarig orosfaktor i både tryckvattenreaktorer och kokvattenreaktorer. Den specifika miljön i kärnkraftstillämpningar består av höga temperaturer och tryck som tillsammans med strålningsfältets inverkan på kylvattnets kemi ger tuffa förhållanden för de material som används i vissa av applikationerna. Det är därför viktigt att förbättra förståelsen av korrosionsprocessen och att få ökad kännedom om hur kylvattnets kemi påverkar de kromoxidbildande nickelbaslegeringarna som används i lättvattenreaktorer.

Detta projekt behandlar atomistisk modellering av väsentliga sensibiliseringsprocesser som skulle kunna bidra till spänningskorrosionssprickor hos lastbärande nickelbas-legeringar i vissa kärnkraftstillämpningar.

Resultat

En sensibiliseringsprocess har formulerats och validerats med hjälp av täthetsfunktionalteori, för kromoxidbildande nickelbaslegeringar vilka normalt används för såväl sin hållfasthet som korrosionsförmåga.

Det skyddande kromoxidskalet utsätts för upplösning av kromoxid såväl som intermittent mikrosprickbildning, där läkning sker genom utåtriktad diffusion av Cr längs legeringens korngränser till Cr-utarmade områden såsom sprickspetsar. Korrosion uppstår om Cr inte tillförs från legeringen. Detta kan bero på Cr-utarmning framför sprickspetsen in i oxiden eller på minskad rörlighet hos kromatomerna i legeringen.

I denna studie beskrivs hur vatten kan fungera som oxidationsmedel för krom i nickelbaslegeringar, förutsatt att vattenmolekyler når gränsytan mellan metall och oxid. Här bildas ny oxid samtidigt som väte antingen avges som vätgas, som hydridjoner i oxidskalet, eller införlivas i legeringen. I det senare fallet tenderar väte att sätta sig i anslutning till atomvakanser i legeringen, vilket minskar dessas rörlighet. Denna reaktionsväg blir viktig då den kromutarmade oxidbeläggningen, som huvudsakligen består av nickeloxid, lätt omvandlas till nickelhydroxid, vilket underlättar vattentransporten till reaktionszonen bortom sprickspetsen. Här undertrycks vätgasutvecklingen på grund av det begränsande lokala utrymmet. Därmed gynnas istället väteupptagningen i legeringen. Sensibilisering för spänningskorrosion uppstår eftersom minskad utåtriktad diffusion främjar intern oxidation av krom. De kvantkemiska beräkningarna understöds av den kvalitativa elektrokemiska Wagnerteorin för bland annat storleksordningsuppskattningar.

Slutligen diskuteras litiums inverkan på korrosion. Litium sätts till kylvattnet för att stabilisera dess kemi, främst dess pH. Studien pekar på att litiums kemi med nickeloxihydroxidskiktet liknar den för väte men att inverkan av litium är mer skadlig på grund av den mer joniska karaktären i [Li-O]- jämfört med den i [H-O]-.

Relevans

Kunskap om de miljösensibiliserande processer som påverkar lastbärande nickelbaslegeringar som är känsliga för spänningskorrosion är avgörande för att långsiktigt öka strålsäkerheten vid kärnkraftverk. SSM har bidragit till utvecklingen av modeller som ökar förståelsen för miljösensibilisering av nickelbaslegeringar i både BWR och PWR. Genom att finansiera en grupp forskare vid Chalmers tekniska högskola har SSM också bidragit till att upprätthålla nationell kompetens inom strålsäkerhet.

Behov av vidare forskning

Denna rapport ger en teoretisk grund för vidareutveckling av modeller som kan bidra till att utveckla bättre nickelbaslegeringar för kärntekniska tillämpningar på lång sikt.

Projektinformation

Kontaktperson SSM: Elena Calota
Referens: SSM2021-7174/ 4530060

SSM perspective

Background
Stress corrosion cracking (SCC) in load bearing structures has been a longstanding issue both in pressurized and boiling water reactors. The specific environment in nuclear power applications consists of high temperatures and pressures that together with the effects of the radiation field on the coolant composition provide tough conditions for the materials used in some of the applications. Thus, it is important to improve the understanding of the corrosion process and to gain insight regarding the effect of coolant composition on the chromia forming nickel-base alloys that are used in Light Water Reactors.

This project concerns first principles atomistic modelling of essential sensitizing processes that would render load bearing nickel-base alloys prone to stress corrosion cracking in nuclear power applications.

Results
A sensitization process has been proposed and validated by means of density functional theory, for the chromia forming nickel base alloys that are usually used for strength as well as corrosion resilience.

The protective chromia scale is subject to chromate dissolution as well as intermittent microcracking, where healing is provided by outward diffusion of Cr in the alloy grain boundaries to Cr depleted regions such as crack tips. Corrosion ensues if Cr is not supplied by the alloy. This may be owing to Cr depletion in front of the crack tip into the oxide or by Cr mobility mitigation in the alloy.

In this work, the researchers articulate possible reaction pathways for water, as oxidizing agent, accessing the metal/oxide interface as well as the fate of hydrogen, either as $H2(g)$, as hydrides ions in the oxide scale, or being incorporated in the alloy. In the case of the latter, hydrogen is preferentially accommodated adjacent to alloy atom vacancies thus mitigating their mobility. This reaction channel becomes important because the Cr depleted oxide scale readily conveys water, by nickel oxide converting into nickel hydroxide, to the reaction zone beyond the crack tip, where chromium becomes oxidized. There, the H2 evolution reaction becomes suppressed owing to the confining environment, and therefore hydrogen pick-up in the alloy becomes enhanced. Sensitization toward SCC ensues as mitigation of outward diffusion of chromium favors internal oxidation. These processes are elucidated by means of the electrochemical Wagner theory for order of magnitude assessment.

Finally, the impact of lithium to corrosion is addressed and support is found for the chemistry of lithium with the nickel oxy-hydroxide scale mirroring that of hydrogen, yet being more detrimental owing to a more ionic nature of the [Li-O]- bond as compared to the [H-O]- bond.

Relevance
Knowledge of the environmental sensitizing processes that affect load bearing nickel-base alloys prone to stress corrosion cracking is essential in order to increase radiation safety at nuclear power plants in the long term. SSM has contributed to the development of models that increase the understanding of environmental sensitizing of nickel-base alloys in both BWR and PWR. Through funding a group of researchers at Chalmers University of Technology, SSM has also contributed to the maintenance of national competence within nuclear radiation safety.

Need for further research
This report provides a theoretical foundation for further development of models that could help develop better nickel-base alloys for nuclear applications in a long term.

Project information
Contact person SSM: Elena Calota
Reference: SSM2021-7174/ 4530060

Sammanfattning

Spänningskorrosion i lastbärande konstruktioner har länge utgjort en betydande orosfaktor i lättvattenreaktorer. Denna korrosion är en följd av de rådande driftförhållandena, som innefattar höga temperaturer och tryck samt strålningsfältets inverkan på kylvattnets kemi.

I detta projekt formuleras och valideras, med hjälp av täthetsfunktionalteori, en sensibiliseringsprocess för spänningskorrosion i kromoxidbildande nickelbaslegeringar, som används för sin hållfasthet och korrosionsbeständighet. Det skyddande kromoxidskalet utsätts för både upplösning av kromoxid och intermittent mikrosprickbildning, där läkning sker genom utåtriktad diffusion av krom längs legeringens korngränser till kromutarmade områden, såsom sprickspetsar. Spänningskorrosion uppstår om krom inte tillförs från legeringen i tillräckligt hög omfattning och tillräckligt snabbt, vilket kan bero på kromutarmning framför sprickspetsen i legeringen eller minskad rörlighet hos kromatomerna i legeringen.

I denna studie beskrivs hur vatten kan fungera som oxidationsmedel för krom i nickelbaserade legeringar, förutsatt att vattenmolekyler når gränsytan mellan metall och oxid. Här bildas ny oxid samtidigt som väte antingen avges som vätgas, som hydridjoner i oxidskalet, eller införlivas i legeringen. I det senare fallet tenderar väte att sätta sig i anslutning till atomvakanser i legeringen, vilket minskar dessas rörlighet. Denna reaktionsväg blir viktig då den kromutarmade oxidbeläggningen, som huvudsakligen består av nickeloxid, lätt omvandlas till nickelhydroxid, vilket underlättar vattentransporten till reaktionszonen bortom sprickspetsen. Här undertrycks vätgasutvecklingen på grund av det begränsande lokala utrymmet. Därmed gynnas istället väteupptagningen i legeringen. Sensibilisering för spänningskorrosion uppstår eftersom minskad utåtriktad diffusion främjar intern oxidation av krom. De kvantkemiska beräkningarna understöds av den kvalitativa elektrokemiska wagnerteorin för bland annat storleksordningsuppskattningar.

Slutligen diskuteras litiums inverkan på korrosion. Litium sätts till kylvattnet för att stabilisera dess kemi, främst dess pH. Våra fynd pekar på att litiums kemi med nickeloxihydroxidskiktet liknar den för väte men att inverkan av litium är mer skadlig på grund av den mer joniska karaktären i $[\text{Li-O}]^-$ jämfört med den i $[\text{H-O}]^-$.

Abstract

High temperatures and pressures, jointly with effects of radiation field on coolant composition define the conditions that cause corrosion in Light Water Reactors. Stress corrosion cracking (SCC) in load bearing structures has been a longstanding issue both in pressurized and boiling water reactors.

Here, a sensitization process is proposed, and validated by means of density functional theory, for the chromia forming nickel base alloys that are resorted to for strength as well as corrosion resilience. The protective chromia scale is subject to chromate dissolution as well as intermittent microcracking, where healing is provided by outward diffusion of Cr in the alloy grain boundaries to Cr depleted regions such as crack tips. Corrosion ensues if Cr is not supplied by the alloy. This may be owing to Cr depletion in front of the crack tip into the oxide or by Cr mobility mitigation in the alloy.

In this work, we articulate possible reaction pathways for water, as oxidizing agent, accessing the metal/oxide interface as well as the fate of hydrogen, either as $H_2(g)$, as hydrides ions in the oxide scale, or being incorporated in the alloy. In the case of the latter, hydrogen is preferentially accommodated adjacent to alloy atom vacancies thus mitigating their mobility. This reaction channel becomes important because the Cr depleted oxide scale readily conveys water, by nickel oxide converting into nickel hydroxide, to the reaction zone beyond the crack tip, where chromium becomes oxidized. There, the H_2 evolution reaction becomes suppressed owing to the confining environment, and therefore hydrogen pick-up in the alloy becomes enhanced. Sensitization toward SCC ensues as mitigation of outward diffusion of chromium favors internal oxidation. These processes are elucidated by means of the electrochemical Wagner theory for order of magnitude assessment.

Finally, the impact of Lithium to corrosion is addressed and support is found for the chemistry of lithium with the nickel oxy-hydroxide scale mirroring that of hydrogen, yet being more detrimental owing to a more ionic nature of the $[Li\text{-}O]^-$ bond as compared to the $[H\text{-}O]^-$ bond.

Content

1. Introduction

This project concerns first principles atomistic modelling of essential sensitizing processes that would render load bearing nickel-base alloys prone to Stress Corrosion Cracking (SCC) in nuclear power applications.

SCC, while apparently generic at first glance, in fact includes aspects that are as unique to the particular environment as they are crucial for structural integrity of the particular component. This commonly necessitates finetuning the match between environmental conditions and the load bearing alloy of choice. Yet, any quest for fundamental understanding must balance between what is generic and what is specific. In this project, this balance is ensured by resorting to atomistic modelling by means of density functional theory thus simultaneously connecting the electronic, chemical and materials aspects via the electronic structure calculations.

SCC in load bearing structures has been a longstanding issue in light water reactors (LWRs). Indeed, stresses owing to high temperatures and pressures jointly with effects of radiation field on coolant composition define the conditions that causes corrosion in LWRs components. In piping, fuel spacers as well as welds, the chromia forming nickel-based alloys are resorted for strength as well as resilience. Besides good mechanical properties, what has made them into the materials of choice is their overall corrosion resistance. Indeed, the choice of alloys – while the LWR coolant control is mainly tuned for power performance and deposit mitigation, the water chemistry to some extent also being affected by fission products – is mainly in response to the enhanced oxidation owing to radiation field induced OH radicals.

We understand oxides on such load bearing nickel-base alloys to intermittently undergo microcracking. Correspondingly, these chromia forming alloys are made to sustain outward diffusion of chromium to the crack tip whereby the crack is healed. If Cr is not supplied, either owing to depletion of Cr or mitigation of outward diffusion of Cr then corrosion ensues. This project concerns the latter case and as owing to hydrogen pick-up. Besides hydrogen, we evaluate the similarity of Li^+ acting H^+ where the former is neither able to undergo the equivalents of hydrogen pick-up in the alloy nor hydrogen evolution. Thus, potentially enriching in the oxide grain boundaries (GB) and crack tips and possibly acting as a tracer of protons in the alloy.

The aim of this work is to articulate and quantify further a sensitization mechanism for hydrogen guided internal oxidation of Ni-base alloy grain boundaries beyond the crack tip of the chromia scale by means of first principles calculations based on density functional theory. Thus, our specific objectives are to model and quantify:

a. hydrogen pick-up in the alloy across the alloy/oxide interface at the crack tip, the so-called water conveyer mechanism,
b. Li^+ acting H^+ equivalent at the oxide crack tip, thus serving as a potential “smoking gun” in our mechanism,

c. hydrogen-controlled vacancy mobility in the alloy as well as mitigation of Cr activity along alloy grain boundaries towards the crack tip,
d. decohesion of alloy grains owing to oxidation along grain boundaries.

2. SCC modelling considerations

Load-bearing metal components are primarily made from ductile alloys to resist stress-induced cracking. However, material selection based solely on inherent mechanical properties is often insufficient under real-world service conditions. To resist combined chemical and mechanical stresses, competitive alloys are tailored to develop a protective oxide scale that (a) prohibits rapid consumption of the alloy by oxidation, and (b) acts barrier against e.g. internal oxidation, nitridation, and hydride formation that are all in different ways detrimental*, vide infra*. The longevity of the oxide scale is determined by its tendencies to dissolve or spall. Continuous or repeated scale healing following dissolution or intermittent spalling, cause depletion of scale former in the alloy that eventually leads to catastrophic corrosion. This stage is often preceded by load induced component failure due to loss of structural integrity, i.e., stress corrosion cracking (SCC). This, owing to loss of ductility in the alloy, is a result of chemical transformations in the alloy. In a series of studies, we have addressed various chemical processes that would precede the SCC.

Building on these, the aim of the present study is to describe how repeated oxide scale cracking and healing in chromia forming nickel base alloy drive hydrogen pick-up and how this may render it vulnerable to SCC.

To understand the impact of stress on scale growth we follow [1] to obtain

$$\frac{\partial X}{\partial t} = \frac{\Delta\mu}{RT} D_{eff} \frac{1}{X} \qquad \text{Eq. 1}$$

$\Delta\mu$ being the chemical potential difference driving the scale growth, R is the gas constant, T is temperature, D_{eff} is the effective diffusivity controlling the scale growth rate, X is the instantaneous scale thickness. Let the diffusivity take a basic Arrhenius form reflecting an intrinsic activation energy E_A and include a spring energy associated contribution of the form $\frac{1}{2}kX^2$ that increases with oxide thickness, i.e,. We write

$$D_{eff} = D_0 e^{-\frac{E_A + \frac{1}{2}kX^2}{RT}} \qquad \text{Eq. 2}$$

Such a spring energy could result from build-up of space charge in the scale or grain boundary density decrease. In case of the latter, such a loss of GB density could come about by some grain boundaries becoming blocked during scale growth. Here, possibly owing to hydrogen pick-up suppressing mobility of scale former. Under such conditions, the scale thickness evolution deviates from its ideal parabolic form

$$X(t) = Ct^{0.5} \qquad \text{Eq. 3}$$

Instead, it becomes increasingly sub-parabolic with time

$$X(t) = C\left[\frac{1}{\mathrm{a}}\ln[1 + at]\right]^{0.5} \qquad \text{Eq. 4}$$

It is noted that at very early stages (when *t* is small) the two expressions become equal. Decelerated scale growth, as compared to the purely parabolic, implies an increasingly attenuated electrochemical potential gradient across the oxide scale. This attenuation in turn results in an increased electrochemical stress that would support scavenging local chemical processes, thereby rendering the scale vulnerable to local spalling [1,2]. Here, we take the interplay between

(i) reoccurring scale failing and scale healing owing to the intrinsic build-up of stress in the scale, and
(ii) external mechanical stresses

to jointly cause the stress induced corrosion that precedes the stress corrosion cracking.

A hallmark of a protective oxide scale is its decelerating mass gain as scale thickness increases. This contrasts with corrosion, where the oxidation rate remains independent of oxide thickness. Passivation is achieved by incorporating scale forming elements such as chromium, aluminium, or silicon in the alloy. These elements react readily with an oxidizing environment to form a continuous, well-adherent, and slow-growing oxide scale that shields the underlying metal from rapid degradation. Nonetheless, protective oxide scales may fail when stress/strain at the alloy/oxide interface surpasses the scale adherence forces, this leading to spallation. Thermal cycling can further compromise the scale, as it develops through quasi-steady-state temperature dependent transport processes that are driven by the temperature-dependent electrochemical potential difference across the scale.

Repeated scale failure and regeneration, besides maintaining a high effective oxidation rate, inevitably reduces the alloy's resistance to oxidation and potential component failure owing to loss of scale former. A limiting such case is the so-called para-linear kinetics [3] that describes the net rate of scale growth to be composed of a growth-rate term that is inversely proportional to scale thickness (passivating) and a constant scale loss-rate term

$$\frac{dX}{dt} = \frac{k_p}{X} - k_s \qquad \text{Eq. 5}$$

Where

$$k_p = \frac{\Delta\mu}{\mathrm{RT}}\, D_{eff} \qquad \text{Eq. 6}$$

$$D_{eff} = D_0 e^{-\frac{E_A}{RT}} \qquad \text{Eq. 7}$$

$$\Delta\mu \propto -RTln\left[\frac{K_{eq}}{Q}\right] \qquad \text{Eq. 8}$$

$$k_s \propto -ln\left[\frac{K_{eq,s}}{Q_s}\right] e^{-\frac{E_{A,s}}{RT}} \qquad \text{Eq. 9}$$

$\Delta\mu$ is the chemical potential difference driving the scale formation, $D_{eff}$is the diffusion constant that controls the equilibration rate, E_A ($E_{A,s}$) being the apparent activation energy for the diffusion (scale dissolution/vaporization), K_{eq} ($K_{eq,s}$) is the equilibrium constant and Q (Q_s) is the corresponding reaction quotient that reflects the instantaneous activities of scale forming (scale dissolving/vaporizing) reactants and products at temperature T. During early stages of oxidation, when X is small, the scale-growth term dominates. As X increases, the thickness-growth term decelerates until it becomes equal to the scale-loss rate. We reach

$$\frac{dX}{dt} = 0 \qquad \text{Eq. 10}$$

i.e., the net scale growth becomes zero, and correspondingly

$$\frac{k_p}{X_{lim}} = k_s \qquad \text{Eq. 11}$$

e.g., due to dissolution or vaporization. Rearranging Eq. 11 we highlight that

$$X_{lim} = \frac{k_p}{k_s}\,. \qquad \text{Eq. 12}$$

Hence, a constant loss-rate of scale former $\frac{k_p}{X_{lim}}$ for a corresponding constant scale thickness is implied. As scale former activity is reduced e.g. owing to depletion, the scale growth-rate term controlled by Q through $\Delta\mu$ in k_p, see Eq. 8, will slow down. Thus, the thickness-independent scale degradation/dissolution process with effective scale loss rate k_s, will eventually leave the load bearing component unprotected to corrosive attacks. This overall understanding is summarized in Figure 1.

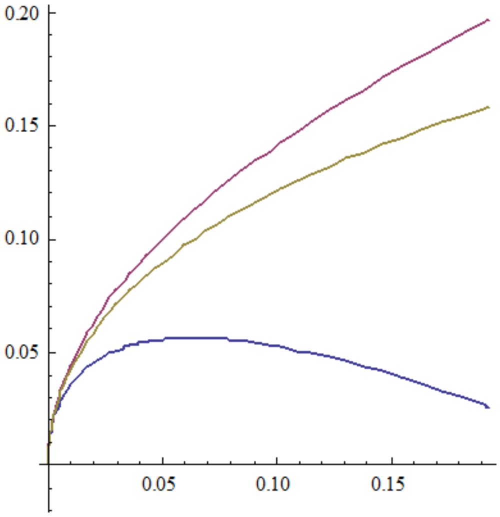

Figure 1. Mass change curves. Top is parabolic mass gain in absence of dissolution/vaporization term, i.e. $k_s = 0$ in Eq. 5. Second is mass gain of oxide scale in presence of dissolution/vaporization term. Bottom is total mass change in presence of dissolution/vaporization term.

Reactive elements, such as Zr, Hf, Y, La, can support adherence and slow growth of oxide scales at high temperatures. They help maintain oxygen activity at the metal-oxide interface at the dissociation pressure, thereby preventing oxygen supersaturation that would otherwise lead to internal oxidation. These reactive elements, when ending up in the oxide scale upon oxidation, occupy oxide grain boundaries due to their aliovalent nature [1,4]. There, their high oxygen affinity renders oxygen vacancies, *a priori* enriched in the grain boundaries, expelled into the lattice where they become dispersed and acquire higher activation energies for diffusion, cf. Eqs. 6-8. Thus, transport in the oxide grain boundaries, that commonly act highways for electrons and anions across the scale owing to high concentration of defects, is mitigated and thereby the scale growth rate decelerates, see Figure 2. Evidence for this interpretation emerges from studies of grain boundary density attenuated scale growth [1].

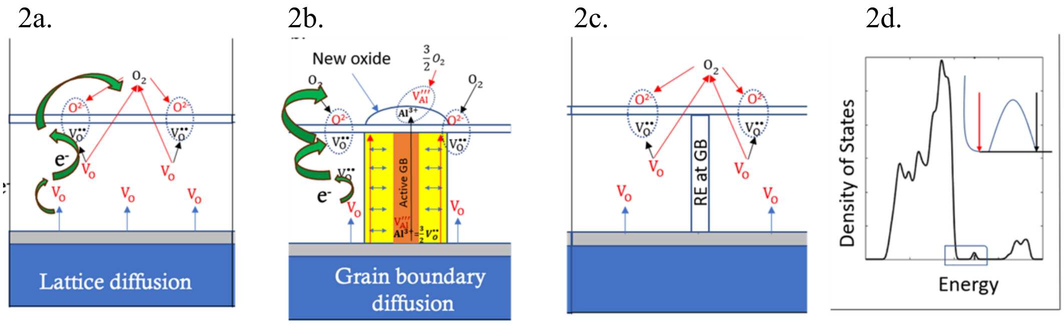

Figure 2 **a-c:** Schematics for three phases of oxidation of alumina formers. Cathode process (top), anode process (bottom). Alloy depicted in blue, inward growing defective alumina front in gray, oxide lattice in white. Red arrows represent electron transport, black arrows represent $V_O^{\bullet\bullet}$ and Al^{3+} transport. **a:** Lattice mediated oxidation of alumina former. **b:** short-circuiting "active" grain boundary including lateral Schottky defect association/dissociation equilibria and interconversion between $\frac{3}{2}V_O^{\bullet\bullet}$ and Al^{3+}. Any incomplete annihilation of $V_O^{\bullet\bullet}$ and O^{2-} causes formation of cationic vacancies that sustain outward oxide growth as manifested in initial formation of oxide ridges. The orange zone contains the manifold of unique grain boundaries. It is in turn contained by the generic exterior zone in yellow that corresponds to the grain boundary width. **c**: RE decoration of GBs effectively expels $V_O^{\bullet\bullet}$ from the GBs, thereby mitigating the $V_O^{\bullet\bullet}$ mediated electron transport and correspondingly also the V_O mobility. **d:** Generic density of states of alumina in presence of oxygen vacancies. Inset: Impurity state in band gap offering electron conductivity is enlarged. Black arrow: E_F in vicinity of alloy/oxide interface: V_O. Red arrow: E_F - in vicinity of gas/oxide interface: $V_O^{\bullet\bullet}$.

In corrosive environments, passivation may become compromised by the interplay of stress, scale formation, and detrimental parallel processes such as hydrogen [4], oxygen and nitrogen uptake [5], and chloride [6] or sulphide [7] accumulations at the alloy/oxide interface, the latter two promoting scale spallation, cf. Figure 3. These are all piggyback processes that ride on the highly exergonic scale formation reaction.

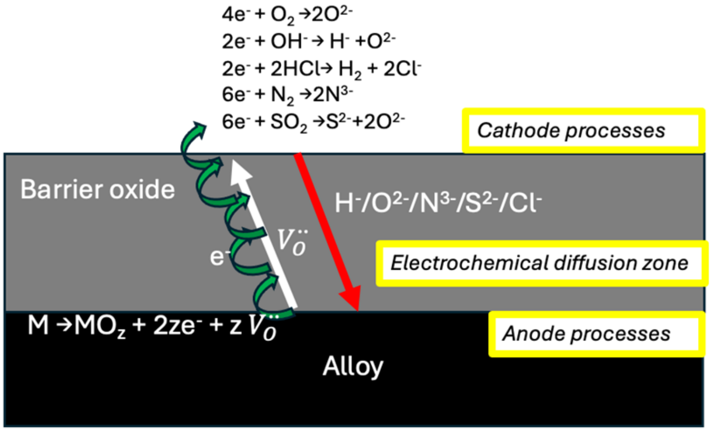

Figure 3. Piggyback processes riding on inward oxide growth channel of barrier oxide. At the metal/oxide interface: Charged oxygen vacancies and electrons are generated owing to the metal oxidation. White arrow: Charged oxygen vacancies diffuse along the oxygen activity gradient from low at alloy/oxide interface to high at the outer oxide surface. Green arrows: Electron hopping between impurity states in the band gap offered by the charged oxygen vacancies, from anode at alloy/oxide interface to cathode at outer surface. Red arrow: inward diffusion of anions utilizing the outward flux of charged oxygen vacancies to form oxy-hydrides, oxy-nitrides, oxy-sulphides, or oxy-chlorides.

As temperatures lower, suppressed cooperative chemical processes gain prominence, especially in water-containing environments. Oxidation by water at lower temperatures, in turn, may lead to hydrogen uptake. This process is facilitated by hydration of the oxide scale and precipitates therein [7,8]. Hydroxylated oxide grain boundaries convey the water-equivalents to the alloy/scale interface where the cathodic proton reduction reaction takes place [7]. There, proximity to the alloy in conjunction with the confining surrounding renders the hydrogen pick-up process able to compete with the cathodic hydrogen evolution reaction [9,10], see Figure 4.

4A	4B	
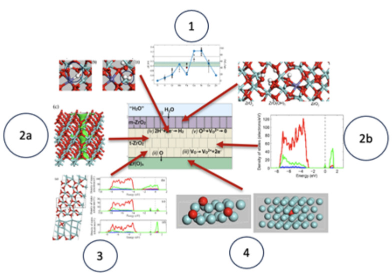	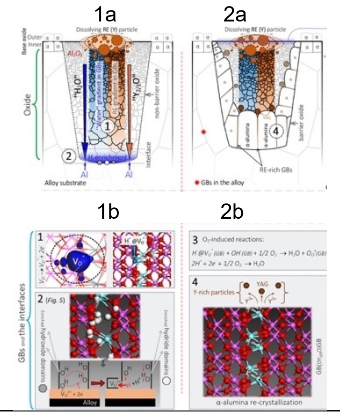	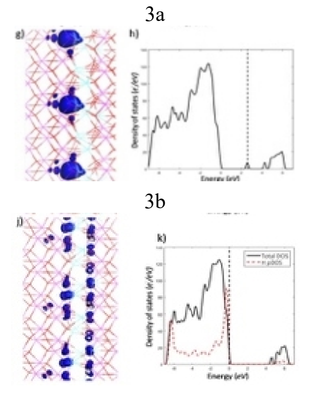

Figure 4. Generic characteristics of oxidation of alloys by water and fates of hydrogen from studies on (4A) zircaloy [8–10] and (4B) FeCrAlY [2]. (4A1) demonstrates hydrogen evolution channel suppressed for Co and Ni in m-ZrO_2 scale. (4A2a) describes an oxygen vacancy pore opening across the t-ZrO_2 barrier oxide pre-transition, due to vacancy coalescence thus explaining avalanching hydrogen pick-up (HPU) fraction at this stage. (4A2b) is the electronic impurity band owing to HPU pore. (4A3) is electronic characteristics in vicinity of the alloy/oxide interface. (4A4) is dissolution of oxygen at interstitial sites in hexagonal Zr. (4B1a) is schematic representation of initial alumina scale formation. (4B1b) zooms in on Y and OH^- co-decorations of alumina grain boundary (GB). (4B2a) is ripened alumina scale. (4B2b) zooms in on Y alumina GB. (4B3a) is the electronic impurity band owing to oxygen vacancies in Y decorated GB. (4B3b) shows removal of impurity states at GB resulting from hydrogen incorporation in oxygen vacancies.

Here, it may be useful to provide an order-of-magnitude assessment of the potential significance of hydrogen uptake in chromia-forming nickel-based alloys near the fuel, such as in spacer grid materials. Assume oxidizing conditions near the fuel with an oxygen partial pressure of approximately 10% due to water radiolysis. Additionally, assume that the chromium dissolution process under in-reactor conditions (300°C and 75 bar) is comparable to that at 600°C under atmospheric pressure. Experimental apparent activation energies (E_A:s) range from 90-100 kJ/mol [3,11], while we estimate an E_A=83 kJ/mol lower bound from DFT calculations [12]. In case of the latter, we have k_s=6.87 10^{-11} cm/s at 600 ^{o}C. Consider the rate of Cr loss from 1cm^2 of scale surface. Let the pre-exponential factor be the same as that for high temperatures, i.e. $\sim 10^{-4.6}$ cm/s for apparent E_A=93 kJ/mol. Let the apparent activation energy at 300 ^{o}C be the lower limit: E_A=83 kJ/mol

$$k_s\,(300\ ^oC, 1\ \mathrm{cm}^2) = 10^{-4.6}\ \cdot e^{-\frac{83000J}{573R}}\,cm^3/s \qquad \text{Eq. 13}$$

From the chromia density (5.22 g/cm^3), molar mass (152 g/mol) and 2 Cr per mol Cr_2O_3

$$k_s(300\ ^oC, 1\ \mathrm{cm}^2) = 2\cdot 10^{-4.6}\cdot e^{-\frac{83000J}{573R}}\cdot\frac{5.22}{152}\frac{mol}{s}Cr \qquad \text{Eq. 14}$$

That is

$$k_s(300\ ^oC, 1\ \mathrm{cm}^2) = 10^{-13.3}\frac{mol}{s}Cr \qquad \text{Eq. 15}$$

Taking 1 year to be $10^{7.5}$s

$$k_s(300\ ^oC, 1\ \mathrm{cm}^2) = \ 10^{-5.8}\frac{mol}{year}Cr \qquad \text{Eq. 16}$$

Number of Cr atoms leaving from 1cm^2 surface

$$k_s(300\ ^oC, 1\ \mathrm{cm}^2) = 10^{-5.8}\cdot 6.022\ 10^{23}\frac{atoms}{year} = 10^{18}\frac{atoms}{year}Cr \qquad \text{Eq. 17}$$

Assume that alloy grain boundaries deliver Cr atoms without forming voids. Let the alloy grain boundary area of 1 μm depth be $4cm\ 1\mu m = 4\ 10^8$Å 10^4 Å $= 4\ 10^{12}$ Å^2. Let the space of a Cr vacancy be one pre Å^2. Then, the growth rate D of the said grain boundary delivering the chromium atoms becomes

$$D(300\ ^oC, 1\ \mathrm{cm}^2) = 2.5\cdot 10^5\ \mu m/year \qquad \text{Eq. 18}$$

For 10^2 alloy grain boundaries (1mm^2 facets) contributing to the Cr loss per 1 cm^2 surface area, we estimate $D = 2.5\cdot 10^3\ \mu m/year$, while for 10^6 alloy grain boundaries (10x10 μm^2 facets) we estimate $D = 0.25\ \mu m/year$. For 1/3 Cr atoms per Å^2 along the alloy grain boundary, the numbers should be multiplied by 3 etc. If the alloy grain boundaries that contribute as source of Cr are 2 atoms wide, the depth of the Cr source is reduced by a factor of 2, etc. These orders of magnitude assessments suggest that over 40 years of service, the impact of chromium loss from alloy 690 impacts several tens of micrometers into the alloy.

Now, consider that for radiolysis assisted Cr oxidation by water we have:

$$2Cr(s) + 3H_2O(l) \rightarrow Cr_2O_3(s) + 6H(abs) \qquad \text{R 1}$$

This implies that for 33% hydrogen pick-up fraction (HPUF) we have each Cr vacancy to be associated with one hydrogen atom. For 0.33% HPUF, every 100 Cr vacancies would be associated with H, i.e., ~1% Cr activity lowering. Moreover, selective hydrogen pick-up in the alloy may render some transport channels along the alloy grain boundaries blocked. If the Cr loss term remains constant, it implies that some Cr sources must become deeper eventually forcing the alloy grains themselves to become Cr sources as potentially orchestrated by the hydrogen pick-up.

Having justified exploration of viable paths for hydrogen pick-up in chromia formers such as alloy 690 in vicinity of the fuel we note that analogous processes have been experimentally shown to lead to hydrogen diffusion into alloy structures, especially at crack tips, promoting Hydrogen-Induced Cracking (HIC) under low pH and potential [13–16]. According to one inferred mechanism, hydrogen molecules accumulate at inclusions and voids inside the metal. Material failure would then result upon reaching a critical pressure. Also, thermodynamic analysis revealed that hydrogen interacts with the stress field, affecting both the internal energy and entropy of the steel. These alterations could lead to an increased anodic dissolution rate, thereby accelerating the SCC growth rate [17]. This anodic dissolution mechanism is basically a hydrogen-facilitated process.

Despite the relevance of such proposed mechanisms in explaining HIC, they primarily rely on macroscopic evidence of specimens that are provoked to undergo severe changes in the alloy microstructure under experimental conditions. Moreover, due to the multiscale complexity of SCC phenomena, it is still not clear from these experiments how the diffusion of hydrogen into the alloy, i.e., hydrogen pick-up, is related to oxidation reactions involved in the stress corrosion of oxide scales in load-bearing alloys. With the work presented in this report, we attempt to provide one such connection by means of first principles atomistic simulations.

Once absorbed by the alloy, hydrogen interacts with microstructural defects, such as grain boundaries, which exacerbates stress corrosion cracking (SCC), particularly intergranular SCC. Although Ni base alloys only absorb a few parts per million of hydrogen on a macroscopic scale [18], hydrogen's affinity for defects—often concentrated at alloy grain boundaries—can lead to hydride precipitation [19,20]. Stress-induced hydrogen accumulation interacts with dislocations, contributing to a ductile-to-brittle transition [21–27]. This report examines hydrogen's interactions within the alloy microstructure, highlighting various pathways by which hydrogen from molecular water can be transported through oxidized grain boundaries via oxy-hydroxide interfaces, to eventually become absorbed by the alloy.

Hydrogen may immobilize scale-forming additives by pinning vacancies along grain boundaries, thereby suppressing protective scale formation, cf. Eq. 7, to expose the alloy to corrosion attacks by mitigating the passivation process [18]. An analogous such effect is owing to intrinsic chromium carbide precipitates, that are known to exacerbate SCC in chromia-forming alloys where the carbon content is intrinsic to the alloy [19]. Possible interplay of hydrogen pick-up and intrinsic such Cr_3C_2, Cr_7C_3, $Cr_{23}C_6$ precipitates during oxidation of chromium has also been proposed [18].

As to prevent corrosion of fuel cladding in nuclear reactors, lithium hydroxide is commonly added to reactor coolant as an alkaline agent to achieve an optimal pH level. One advantage of lithium hydroxide over other alkaline solutions is due to transparency of lithium-7 to neutrons, which enhances reactor efficiency. However, the continuous addition of lithium hydroxide solutions increases lithium concentration in the reactor coolant, necessitating its removal through an ion exchanger until the desired concentration is reached. Unlike hydrogen, lithium does not have an analogue to the hydrogen evolution reaction. This may result in lithium accumulation within the oxide scale. In fact, lithium ions have been detected in the inner oxide layer of Alloy 690, and some researchers have suggested a potentially harmful effect of lithium on structural materials in the cores of nuclear power plants. [20,21]. This effect could include lithium enrichment at oxide grain boundaries and influence properties at the crack tip.

Understanding of hydrogen's roles in alloy degradation and loss of integrity necessitates examining explicit mechanisms for hydrogen uptake as a by-product of water oxidation. Hydrogen uptake and embrittlement have been studied in the context of light-water reactors (LWR), particularly after long plant operation, approx. 40 years, or even after extending the service of a power plant to 60 er even 90 years. However, most studies rely on accelerated ageing laboratory experiments [22,23] which may not resemble the full complexity of oxidation processes in operating conditions. The hydrogen uptake caused by water oxidation has been mechanistically investigated using density functional theory (DFT) calculations, examining both zirconia [4,10,24,25] and alumina-forming alloys [2,26–28]. Recently, we extended this understanding to include the chromia-forming nickel base alloys like Alloy 690 [29], as summarized more extensively in the current report.

3. Computational details

Spin-polarised calculations were performed based on density functional theory [30,31] in the implementation with plane waves [32] and pseudopotentials using the CASTEP code [33] within the Materials Studio framework. The Perdew, Burke, and Ernzerhof (PBE) GGA functional [34,35] was employed in all calculations. Core electrons were described by on-the-fly generated norm-conserving pseudopotentials [36], and a plane-wave energy cut-off was set to 1200 eV. The *k*-point sampling of the Brillouin zone was made by means of the Monkhorst-Pack scheme [37,38] with a *k*-point separation of 0.05 $Å^{-1}$ for all structures. The electronic structure was minimised until the total energy difference was smaller than 10^{-7} eV/atom for two consecutive SCF cycles. A Gaussian smearing scheme with a width of 0.1 eV was used to facilitate convergency. All structures were fully optimised using the L-BFGS [39,40] algorithm with a total energy convergence tolerance of 10^{-5} eV/atom, maximum force tolerance of 0.03 eV/Å, maximum stress tolerance of 0.05 GPa, and maximum displacement tolerance of 10^{-3} Å.

The initial bulk structures for further geometry optimisations were obtained primarily from the Materials Studio database and the inorganic crystal structure database (ICSD) [41]. Optimised structures were then compared with experimental lattices reported in ICSD, and the percentage error was calculated.

3.1. Nickel oxide lamellae interface model description and relevance to oxide scale growth in light-water reactors (LWR)

Despite that various intergranular (IG) SCC mechanisms have been proposed in the literature, none of them can fully describe the complexity of grain boundary oxidation associated with crack propagation in Ni base alloys [42]. The IGSCC model proposed by Scott [43] links such events and suggests that internal oxidation occurs at grain boundaries. These models are often validated by experiments conducted at temperatures similar to those in Light Water Reactor (LWR) operating conditions. Due to the slow diffusion of reactive solute species, such as chromium (Cr), internal oxidation at grain boundaries proceeds, enabling inward oxygen diffusion [50]. Here, the water conveyance mechanism is posited as a potential driver of oxygen ingress, leading to further internal oxidation of the alloy.

Our modelling approach accounts for oxidized grain boundaries, with NiO being the predominant oxide in Ni base alloys. We model NiO growth along grain boundaries by increasing the number of nickel atom layers in the [111] growth direction, which also promotes the stacking of $Ni(OH)_2$. The growth of NiO at the oxide scale can also occur by condensation reactions that transform $Ni(OH)_2$ into NiO and H_2O, producing an intercalation compound, as illustrated schematically in Figure 5. This figure also shows that NiO particles at the oxide scale can undergo hydrolysis reactions, supporting the role of the water conveyance mechanism at oxy-hydroxy interfaces, which we will discuss further in the following sections.

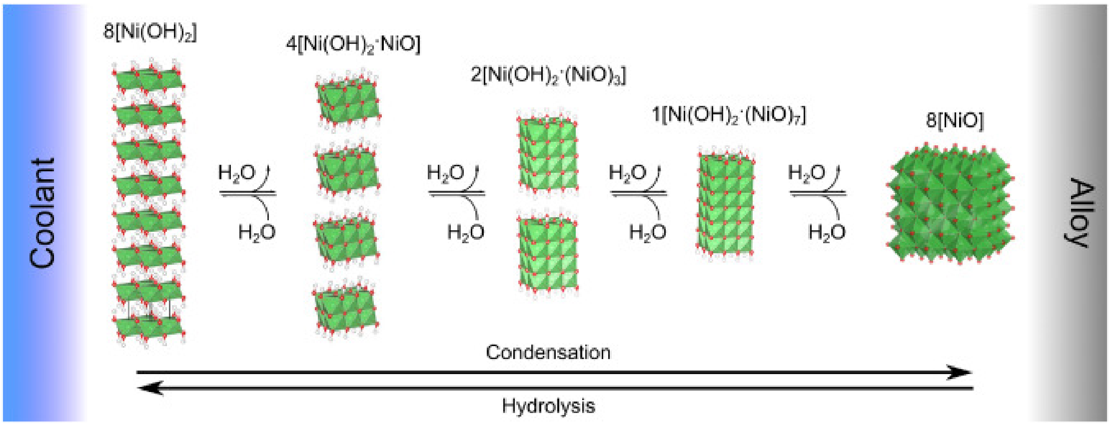

Figure 5. Schematic representation of the condensation of nickel hydroxide (β-Ni(OH)2, left) and the hydrolysis of nickel oxide (rock salt NiO, right) in an aqueous environment in nuclear power plants. Reprinted from [29] Licensed under CC BY 4.0

4. On alloy oxidation by water

As documented in the literature [52,53], Ni base alloys develop a duplex oxide scale, with an outer layer consisting of a complex mixture of $Ni(OH)_2$, NiO, and $NiFe_2O_4$. This layer forms through solid-state transformations of the initial mixed oxide, which primarily consists of $(Ni,Fe)Cr_2O_4$ spinels. The outer oxide layer facilitates the formation of a thin, well-adherent, and compact Cr_2O_3 scale at the interface with the alloy matrix, due to the low effective oxygen partial pressure (pO_2) near the alloy/oxide boundary in the oxidizing environment.

Stress corrosion of the oxide scale exposes the alloy matrix to water molecules at the crack tip, causing further oxidation of the alloy. When conditions for crack healing are met, effective solid-state reactions in the initial complex oxide allow the formation of passivating $NiFe_2O_4$ and $(Ni,Fe)Cr_2O_4$ spinels. However, repeated cracking and healing processes locally deplete chromium near the cracked area. Even though the alloy has an excess of chromium, and water acting as an oxidizing agent is conveyed by hydroxylated/oxidized grain boundaries, the chromium activity at the crack tip becomes insufficient to form a protective oxide scale, as illustrated in Fig. 6.

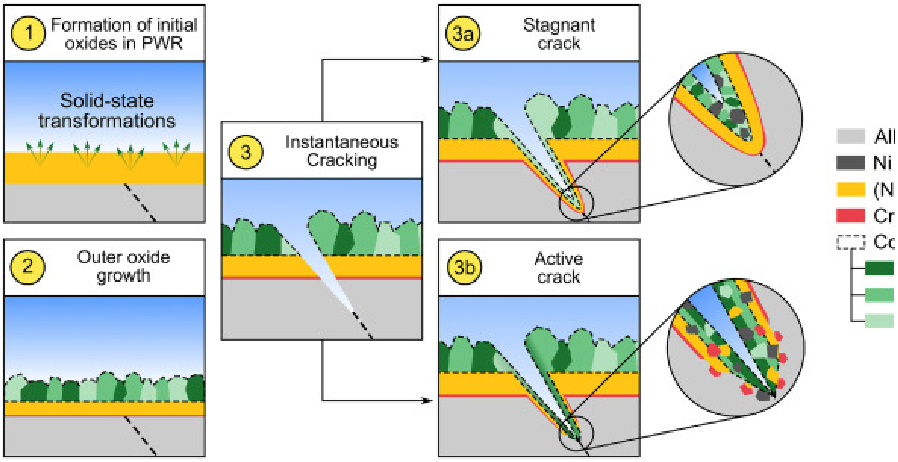

Figure 6. Schematic representation of oxide growth and two types of intergranular cracks observed in Ni base alloys. Reprinted from [29]. Licensed under CC BY 4.0

4.1. On sensitization of alloy grain boundaries in chromia-forming alloys by the water conveyer mechanism as a possible pathway for hydrogen pick-up

Figure 7 summarizes a sequence of reactions occurring at the alloy/oxide interfaces, relevant to stress corrosion cracking (SCC), hydrogen-induced cracking (HIC), and embrittlement in Ni base alloys. These reactions correspond to the scenario depicted in Figure 6(3b), where water is in direct contact with an unprotective “junk oxide” layer, primarily composed of Cr_2O_3, NiO, and $Ni(OH)_2$. This layer provides a short-circuit pathway for chromium oxidation by water, a pathway that also includes oxidized grain boundaries in the Ni base alloys, as described in the literature [30,31,52,53].

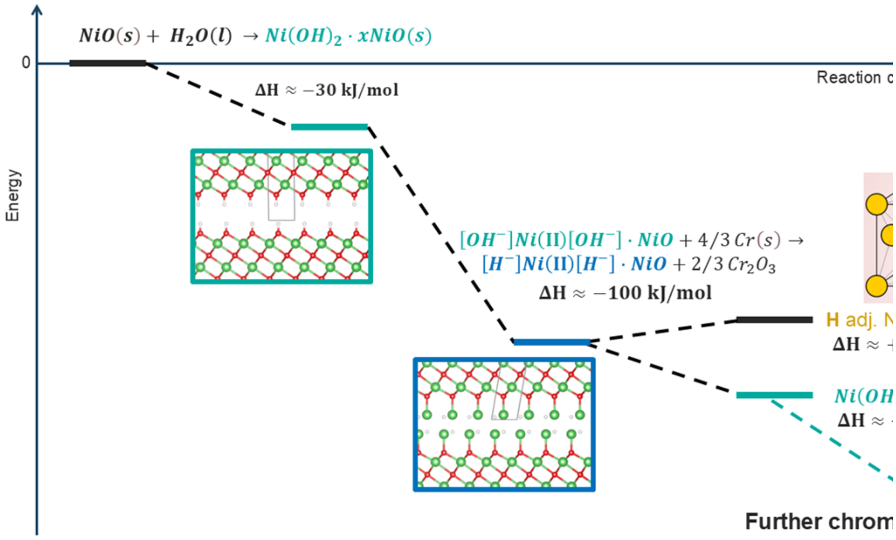

Figure 7. Sequence of reaction involved in the sensitization by hydrogen upon chromium oxidation in Ni base alloys, the water conveyer mechanism. Hydroxylation of NiO particles is taken as the energetic reference for the following reactions at the alloy/oxide scale. The enthalpy formation for the oxy-hydroxide interface is highlighted by the green energy level and its structure by the green box. As oxidant for chromia formation, the interface transforms into an oxy-hydride interface, highlighted in blue. This chemical reaction is understood to be the driver for other chemical events at the alloy/oxide interface. Upon transformation of the oxy-hydride interface, two possible scenarios are highlighted. In yellow, hydrogen uptake by the alloy takes place (yellow spheres represent Ni metal atoms, purple represents hydrogen in a interstitial octahedral site and the empty sphere represents a single metal vacancy); highlighted in green is the hydrogen-catalysed cyclic Ni(0) build-up in NiO having also as a product the oxy-hydroxide interface. The restored oxy-hydroxide interface may further participate in subsequent chromium oxidation reactions.

We demonstrate the viability of the water conveyance mechanism through the transformation of nickel oxide into a nickel oxyhydroxide interface upon reaction with water, an exothermic process releasing approximately 30 kJ/mol. These interfaces subsequently act as oxidizing agents for chromium, supplying oxygen atoms from hydroxyl groups at the interface (effectively oxygen from water molecules). This reaction transforms the interface into an oxy-hydride structure, where protons occupy oxygen vacancies.

The formation of chromia drives further transformations at the alloy/oxide interface. The oxy-hydride interface model represents transient local hydrides that may promote embrittlement or spalling and contribute to stress corrosion of the oxide scale, observed macroscopically as oxide scale loss (spalling). The presence of local nickel hydrides, though unexpected in stable forms in Ni base alloys, has indeed been reported in the literature [54]. Additionally, the authors observed that the hydride phase decomposed after aging samples at room temperature, highlighting the metastable nature of such interfaces.

Due to its transient nature, the oxy-hydride interface may participate in further chemical reactions. In the bottom right of Figure 7, we highlight two distinct pathways involving the reduction of Ni(II), leading to the formation of Ni(0) metal particles within the oxide scale, a phenomenon that has also been observed experimentally [55–57]. Additionally, a third pathway (not shown in Figure 7), the hydrogen evolution reaction (HER), involves the recombination of H^- and H^+ from the oxy-hydride interface. This reaction is mildly endothermic, requiring 20–30 kJ/mol. While HER would typically be spontaneous on open surfaces due to the entropy gain associated with hydrogen evolution at reactor conditions, the confined environment at the alloy/oxide interface negates the translational entropy contribution for $H_2(g)$, thus rendering the reaction kinetically hindered.

Simultaneously, the uptake of hydrogen atoms from the oxy-hydride interface becomes favourable, as these atoms bond to vacancies in the alloy's microstructure. Our results support the likelihood of hydrogen atom enrichment in defect-rich regions within the alloy, such as grain boundaries, crack tips, and metal atom vacancies. Furthermore, the formation of hydrogen-vacancy complexes suppresses vacancy mobility, leading to a reduction in local ductility. In this way, hydrogen also inhibits solute mobility within the alloy, particularly for chromium, which in turn impedes the reformation of the oxide scale needed to counteract chromium dissolution and renew the oxide layer where local spalling has occurred (see Introduction).

Nickel hydroxide has been observed experimentally in the reaction zone throughout all stages of Alloy 690 corrosion [58], underscoring the significance of the water conveyance mechanism for oxidizing chromium. However, when chromium is inaccessible, intermittent standalone nickel oxide/hydroxide transformations can also contribute to local spalling of the oxide scale, thereby relieving the confinement at the alloy/oxide interface. Consequently, the continuous formation of nickel hydroxide may help suppress hydrogen uptake in this alloy, albeit at the cost of increased corrosion.

Finally, we highlight the reaction pathway in which NiO, while transforming into Ni(s), acts as an oxidizing agent to promote chromia formation. This pathway can be activated or catalysed by the presence of hydrogen—specifically, as H^+ in the hydroxylated lamella and as H^- in response to chromium oxidation. The formation of Ni(s) may be further facilitated by the increased effective surface area of NiO due to hydroxylation. This reaction remains catalytic as long as hydrogen is not lost through uptake by the alloy, absorption by the growing Ni particles, or as $H_2(g)$.

In summary, our work offers a comprehensive understanding of key chemical transformations involved in stress corrosion of chromia-forming nickel base alloys, shedding light on the sensitization of alloy grain boundaries, stress corrosion cracking, and hydrogen embrittlement.

4.2. On Li$^+$ acting H$^+$ equivalent in oxidized grain boundaries

In this section, we emphasize the analogy between protons (H$^+$) and lithium cations (Li$^+$). Here, Li$^+$ ions can be understood as a potential "smoking gun" for the proposed water conveyer mechanism and hydrogen pick-up. Consequently, in what follows, we explore the well-established analogous behaviour of H$^+$ and Li$^+$ to illustrate the impact of ion exchange along nickel oxyhydroxide grain boundaries, where OH$^-$ may be partially substituted by OLi$^-$.

The stability of lithiated interfaces is explored by first considering the following solid-state reaction,

$$Li_2NiO_2(s) + 5NiO(s) \rightarrow Li_2NiO_2 \cdot (NiO)_5(s) \qquad \text{R 2}$$

Our first-principles calculation results indicate that the formation of a lithiated interface within NiO is endothermic by approx. 30 kJ/mol. However, this reaction may become exergonic in reactive zones where entropic contributions could create metastable phases, similar to reactions involving hydrogen pick-up discussed in the section above. Indeed, experiments have shown that only metastable phases appear in the phase diagram of Li incorporated into NiO [44].

Following the water conveying mechanism, we subsequently evaluate the ability of the lithiated interface acting as the oxidizing agent for chromia formation. In this reaction, oxygen from the Li-O bond is removed from the interface model, thereby transforming it into an “hydride analogue”. The consumption of oxygen is then used to oxidize Cr(0) into Cr(III) according to the following reaction

$$[OLi^-]Ni(\mathrm{II})[OLi^-] \cdot (NiO)_5 + 4/3\ Cr(s) \rightarrow [Li^-]Ni(\mathrm{II})[Li^-] \cdot (NiC \\ + 2/3\ Cr_2O_3 \qquad \text{R 3}$$

As for the oxy-hydroxide interface, the reaction involving the oxy-lithiated interface as one of the reactants is exothermic by approx. 200 kJ/mol. Therefore, similar conclusions as for the water conveyer mechanism also apply for lithiated interfaces. Although interfaces that incorporate Li(I) are structurally different from the hydroxylated interfaces the rather dramatic changes in the interface structures suggest sensitization of oxide grain boundaries towards stress corrosion in both cases. The lithiated oxy-hydroxy interfaces are, in addition, taken to support sensitization toward stress corrosion cracking by facilitating the water permeation.

Analogous to hydrogen pick-up, we also calculated the reaction energy for lithium pick-up by the alloy. We found this reaction to be exothermic by approximately 30 kJ/mol Li. And where a complex between hydrogen and metal atom vacancy is formed in the alloy, lithium is sufficiently large to be accommodated in the metal atom site.

4.3. The effect of hydrogen in vacancy mobility in nickel

We have shown a possible pathway for hydrogen pick-up in the water conveyer mechanism that is associated with the formation of hydrogen-vacancy complexes in the alloy microstructure, primarily on defect-rich regions. The affinity of hydrogen for metal vacancies in the alloy reported here and in the original publication for the water conveyer mechanism [29] is in accordance with results published elsewhere [45,46]. In the following we show the results from our first-principles simulations for the effect of hydrogen on self-diffusion of Ni, i.e., pinning of vacancies in the alloy caused by hydrogen accumulation, see Figure 8 below.

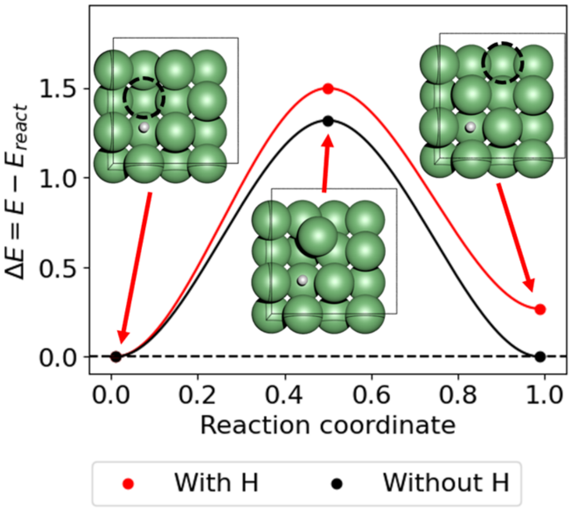

Figure 8. Lowest energy pathway and activation energy and the effect of hydrogen on vacancy diffusion in nickel. Nickel atoms are represented by green spheres, hydrogen by white speres and a vacancy by a dashed empty circle. All energies are normalized by the total energy (in electron volt, eV) of their respective reactants at reaction coordinate 0. The reaction pathway in black is the diffusion of a vacancy without hydrogen (structures not shown) and the pathway in red is the vacancy diffusion with one hydrogen atom is located at the octahedral interstitial site close to a vacancy, i.e., the hydrogen-vacancy complex.

By analysing both reaction pathways in Figure 8, one can see that the hydrogen-vacancy affinity is about 0.3 eV and the dissociation of the hydrogen-vacancy complex is endothermic. The pinning of vacancies is caused by the activation energy that is 0.1-0.2 eV higher in the presence of hydrogen (red pathway) in comparison with the hydrogen-free case (black pathway). Our calculated increase in the activation energy is in accordance with results by Wang and co-workers [45,46]. Such an increase affects atom mobility in the alloy by one order of magnitude (hydrogen pick-up causes atoms to diffuse ten times slower compared to the diffusion in hydrogen-free alloys). As the diffusion of other elements such as chromium or iron are mediated by metal vacancies, one may expect similar effects of hydrogen in the diffusion of these elements in nickel base alloys.

5. Summary and conclusions

The work serves to understand the crack tip oxidation in chromia forming nickel base alloys relevant to the stress corrosion cracking where water is the oxidizing agent, and where water may effectively be conveyed as oxy-hydroxide transients to the oxide/alloy interface to react with chromium forming chromia. It puts emphasis on possible fates of hydrogen that comprises by-product in the oxidation process.

The nickel base chromia forming alloys such as alloy 600 and 690, with 15 and 30 At% chromium, respectively, are tailored to exhibit enduring strength as well as resilience toward corrosion in light water nuclear reactors. A passivating oxide scale results from early irregular nickel iron chromite $(Ni,Fe)Cr_2O_4$ that, on chromate $Cr_2O_4^-$ dissolution owing to further oxidation, is gradually being transformed into non-protective nickel hydroxide $Ni(OH)_2$ and nickel oxide NiO, as well as nickel ferrite $NiFe_2O_4$ that contributes an outer scale that protects an inner increasingly dense, continuous and well-adherent duplex oxide scale composed of $(Ni,Fe)Cr_2O_4$ and chromia Cr_2O_3. The resilience of this protective oxide scale is challenged by sensitization processes towards stress corrosion cracking.

An overall understanding of stress corrosion cracking was provided where Wagner theory was utilized to articulate

- the notion of barrier oxide in the context of alloys that include scale former,
- how stress build-up in oxide scale impacts on oxide scale growth,
- how catastrophic oxidation relates to continuous loss and regeneration of scale former – so-called para-linear oxidation,
- order-of-magnitude assessments of hydrogen pick-up in relation to chromium oxidation and dissolution,
- how piggybacking scavenging processes may utilize the highly spontaneous scale formation be detrimental to the adherence between scale and alloy.

Repeated scale cracking and re-healing requires easily accessible chromium in the alloy, which is mainly conveyed along alloy grain boundaries. This access becomes increasingly challenged with time not exclusively owing to the chromium depletion processes but also due to compound formation involving chromium in the alloy grain boundaries. These may comprise inherent $Cr_{23}C_6$ and Cr_7C_3 chromium carbides, and inward diffusing oxygen along alloy GB:s causing local internal oxidation. Here, possible oxidation-driven hydrogen uptake is taken to infer alloy vacancy pinning. Thus, access of Cr at the crack tip becomes increasingly impeded, while grain boundary oxidation is enhanced and, correspondingly, so is the risk for component failure.

Along these lines, one specific objective of this research project was (a) to elucidate the fates of hydrogen during oxidation of nickel base chromia forming alloys. A second specific objective was (b) to explore to what extent lithium, which is added to the reactor coolant as LiOH(aq) for control of pH, traces the migration of hydrogen.

In case of the **specific project objective a**, the emerging mechanistic understanding is consistent with the following once the oxide scale has become chromium depleted owing to the dissolution of chromates:

- Hydroxylated NiO grain boundaries offer stable steady state moieties in reactions of water with NiO(s) when water is the limiting reactant, which would result from the chromium oxidation at the crack tip.
- Transient nickel oxy-hydroxy-hydrides form upon the nickel oxy-hydroxide moieties serving the oxidation of chromium to produce chromia.
- heterostructures of chromia, nickel metal and nickel oxide result from transients' disproportionation whereby hydrides H^- recombine with protons H^+
    - to produce $H_2(g)$, that is the hydrogen evolution reaction. It is understood to be suppressed in vicinity of the oxide/alloy interface owing to the confinement that it constitutes.
    - to serve catalyst in the reaction where oxidation of chromium by nickel oxide results in formation of metallic nickel particles, explaining why they are found to co-exist with nickel oxide and chromia in vicinity of the crack tip.
    - to become absorbed in nickel metal particles as well as in the alloy, in vicinity of metal atom vacancies.

The coopeting processes, driven by the effective oxidation of chromium by water and as controlled by the fates of hydrogen, provide a unified understanding of the complex oxide composition observed at the crack tip of nickel base chromia formers. The fraction of hydrogen that becomes picked up by the alloy – but not in metallic nickel inclusions in the oxide or evolving as H_2 – is taken to be increasingly detrimental at late stages when access to chromium that is decisive for the passivating oxide scale to form, becomes limited by chromium mobility. This situation is postponed in alloy 690 as compared to alloy 600.

For the **specific project objective b**, we explore the well-known analogous speciation of H^+ and Li^+ to describe the impact of ion exchange along nickel oxy-hydroxide grain boundaries, partially substituting OH^- by OLi^-. It is noted that the two hydroxylated interfaces that form the grain boundary experience increased repulsion on substitutional enrichment of Li+. This is because the ionic contribution is favoured in the bond between O_2^- and Li^+ while the covalent contribution dominates in the bond between O_2^- and H^+. This causes reduced screening of repulsive interface-interface interactions across the oxy-hydroxy grain boundaries upon increased replacement of OH^- by OLi^-. It is taken to support sensitization toward stress corrosion cracking by the lithiated oxy- hydroxy interfaces facilitating water permeation as well as access to the alloy/oxide interface.

Chromium mobility, or more broadly vacancy mobility in Ni-based alloys, was investigated with a focus on the impact of hydrogen uptake resulting from the oxidation of chromium by water, aligning with the **specific project objective c**. From the computed potential energy landscape, transition states, and associated activation energies for diffusion, it is clear that hydrogen binds to alloy vacancies. Low-energy inter-site solute hopping requires the coupled displacement of the vacancy associated with hydrogen. The activation energy for vacancy diffusion increases by 0.1–0.2 eV, thereby slowing solute diffusion rates in the alloy by a factor of 10 to 50.

Lastly, aligned with the **specific project objective d**, we discuss that adherence between alloy and oxidized grain boundaries. Consequently, alloy grain decohesion and spalling of the oxide scale, as well as resilience toward the combined stresses – inherent, from scale growth, and external, from component vibrations – jointly contribute the stress corrosion cracking process. Hydrogen pick-up in vicinity of the alloy/oxide interface may result in repeated local scale cracking/spalling as cause loss of ductility in the alloy at this interface. Also, stress build-up in the scale owing to increased space-charge, scale/alloy orientation mismatch, grain-boundary density dependent scale growth all may render the scale growth square-root-logarithmic sub-parabolic. Both factors, loss of interface ductility and increasingly challenged oxide scale integrity, when combined with externally applied load and vibrations facilitate the intermittent scale failure leaving the alloy repeatedly under attack.

In this work, fundamental electrochemical sensitization processes toward oxide scale de-coherence and stress corrosion cracking were elucidated. By benefitting from these results and methodology in the context of multi-scale modelling, contact should be made with phenomenological structural mechanics-based models to predict the remaining time of service of a structural component.

6. Acknowledgements

This work has been funded and supported by Swedish Radiation Safety Authority (SSM). The computations were performed on resources at Chalmers Centre for Computational Science and Engineering (C3SE) provided by the National Academic Infrastructure for Supercomputing in Sweden.

7. References

[1] C. Geers, I. Panas, Impact of Grain Boundary Density on Oxide Scaling Revisited, Oxidation of Metals 91 (2019) 55–75. https://doi.org/10.1007/s11085-018-9867-0.

[2] N. Mortazavi, C. Geers, M. Esmaily, V. Babic, M. Sattari, K. Lindgren, P. Malmberg, B. Jönsson, M. Halvarsson, J.E. Svensson, I. Panas, L.G. Johansson, Interplay of water and reactive elements in oxidation of alumina-forming alloys, Nat Mater 17 (2018) 610–617. https://doi.org/10.1038/s41563-018-0105-6.

[3] B. Pujilaksono, T. Jonsson, M. Halvarsson, I. Panas, J.-E. Svensson, L.-G. Johansson, Paralinear Oxidation of Chromium in O2 + H2O Environment at 600–700 °C, Oxidation of Metals 70 (2008) 163–188. https://doi.org/10.1007/s11085-008-9114-1.

[4] M. Lindgren, C. Geers, I. Panas, Possible origin and roles of nano-porosity in ZrO 2 scales for hydrogen pick-up in Zr alloys, Journal of Nuclear Materials 492 (2017) 22–31. https://doi.org/10.1016/j.jnucmat.2017.05.017.

[5] C. Geers, V. Babic, N. Mortazavi, M. Halvarsson, B. Jönsson, L.-G. Johansson, I. Panas, J.-E. Svensson, Properties of Alumina/Chromia Scales in N2-Containing Low Oxygen Activity Environment Investigated by Experiment and Theory, Oxidation of Metals 87 (2017) 321–332. https://doi.org/10.1007/s11085-016-9703-3.

[6] V. Cantatore, M.A. Olivas Ogaz, J. Liske, T. Jonsson, J.-E. Svensson, L.-G. Johansson, I. Panas, Oxidation Driven Permeation of Iron Oxide Scales by Chloride from Experiment Guided First-Principles Modeling, The Journal of Physical Chemistry C 123 (2019) 25957–25966. https://doi.org/10.1021/acs.jpcc.9b06497.

[7] H.J. Grabke, D. Wiemer, H. Viefhaus, Segregation of sulfur during growth of oxide scales, Appl Surf Sci 47 (1991) 243–250. https://doi.org/10.1016/0169-4332(91)90038-L.

[8] M. Lindgren, G. Sundell, I. Panas, L. Hallstadius, M. Thuvander, H.-O. Andrén, Toward a Comprehensive Mechanistic Understanding of Hydrogen Uptake in Zirconium Alloys by Combining Atom Probe Analysis With Electronic Structure Calculations, in: Zirconium in the Nuclear Industry: 17th Volume, ASTM International, 100 Barr Harbor Drive, PO Box C700, West Conshohocken, PA 19428-2959, 2015: pp. 515–539. https://doi.org/10.1520/STP154320120164.

[9] M. Lindgren, I. Panas, Impact of additives on zirconium oxidation by water: mechanistic insights from first principles, RSC Adv 3 (2013) 21613. https://doi.org/10.1039/c3ra42941e.

[10] M. Lindgren, I. Panas, Confinement dependence of electro-catalysts for hydrogen evolution from water splitting, Beilstein Journal of Nanotechnology 5 (2014) 195–201. https://doi.org/10.3762/bjnano.5.21.

[11] H. Falk-Windisch, J.E. Svensson, J. Froitzheim, The effect of temperature on chromium vaporization and oxide scale growth on interconnect steels for Solid Oxide Fuel Cells, J Power Sources 287 (2015) 25–35. https://doi.org/10.1016/j.jpowsour.2015.04.040.

[12] I. Panas, J.-E. Svensson, H. Asteman, T.J.R. Johnson, L.-G. Johansson, Chromic acid evaporation upon exposure of Cr2O3(s) to

H2O(g) and O2(g) – mechanism from first principles, Chem Phys Lett 383 (2004) 549–554. https://doi.org/10.1016/j.cplett.2003.11.079.

[13] H. Shirazi, R. Eadie, W. Chen, A review on current understanding of pipeline circumferential stress corrosion cracking in near-neutral PH environment, Eng Fail Anal 148 (2023) 107215. https://doi.org/10.1016/J.ENGFAILANAL.2023.107215.

[14] S.X. Mao, M. Li, Mechanics and thermodynamics on the stress and hydrogen interaction in crack tip stress corrosion: experiment and theory, J Mech Phys Solids 46 (1998) 1125–1137. https://doi.org/10.1016/S0022-5096(97)00054-9.

[15] B. Gu, J. Luo, X. Mao, Hydrogen-Facilitated Anodic Dissolution-Type Stress Corrosion Cracking of Pipeline Steels in Near-Neutral pH Solution, Corrosion 55 (1999) 96–106. https://doi.org/10.5006/1.3283971.

[16] S.X. Mao, B. Gu, N.Q. Wu, L. Qiao, The mechanism of hydrogen-facilitated anodic-dissolution-type stress corrosion cracking: theories and experiments, Philosophical Magazine A 81 (2001) 1813–1831. https://doi.org/10.1080/01418610108216638.

[17] B.T. Lu, L.J. Qiao, J.L. Luo, K.W. Gao, Role of hydrogen in stress corrosion cracking of austenitic stainless steels, Philosophical Magazine 91 (2011) 208–228. https://doi.org/10.1080/14786435.2010.515262.

[18] V. Babic, V. Cantatore, C. Geers, I. Panas, J. Chen, On Water Induced Sensitization of Ni (Fe,Cr) alloys towards Stress Corrosion Cracking in LWR Piping from 1st Principles Modelling, 2021. https://www.stralsakerhetsmyndigheten.se/publikationer/rapporter/sakerhet-vid-karnkraftverken/2021/202102/ (accessed April 3, 2023).

[19] M. Kajihara, M. Hillert, Thermodynamic evaluation of the Cr-Ni-C system, Metallurgical Transactions A 21 (1990) 2777–2787. https://doi.org/10.1007/BF02646072/METRICS.

[20] A.S. Sinjlawi, L. Dong, M. Ickes, K. Sun, G.S. Was, Irradiation assisted stress corrosion cracking of 347 stainless steel in simulated PWR primary water containing lithium hydroxide or potassium hydroxide, Journal of Nuclear Materials 586 (2023) 154676. https://doi.org/10.1016/j.jnucmat.2023.154676.

[21] EPRI, Effect of Boron Concentration on Alloy 690 Corrosion Product Release Rates, Palo Alto, 2001.

[22] W. Kuang, G.S. Was, The effect of grain boundary structure on the intergranular degradation behavior of solution annealed alloy 690 in high temperature, hydrogenated water, Acta Mater 182 (2020) 120–130. https://doi.org/10.1016/j.actamat.2019.10.041.

[23] W. Kuang, G.S. Was, A high-resolution characterization of the initiation of stress corrosion crack in Alloy 690 in simulated pressurized water reactor primary water, Corros Sci 163 (2020) 108243. https://doi.org/10.1016/j.corsci.2019.108243.

[24] M. Lindgren, G. Sundell, I. Panas, L. Hallstadius, M. Thuvander, H.O. Andrén, Toward a Comprehensive Mechanistic Understanding of Hydrogen Uptake in Zirconium Alloys by Combining Atom Probe Analysis With Electronic Structure Calculations, ASTM Special

Technical Publication STP 1543 (2015) 1–25. https://doi.org/10.1520/STP154320120164.

[25] M. Lindgren, I. Panas, Oxygen Vacancy Formation, Mobility, and Hydrogen Pick-up during Oxidation of Zirconium by Water, Oxidation of Metals 87 (2017) 355–365. https://doi.org/10.1007/s11085-016-9695-z.

[26] T. Boll, V. Babic, I. Panas, O. Bäcke, K. Stiller, On aliovalent cations control of α-alumina growth on doped and undoped NiAl, Acta Mater 210 (2021) 116809. https://doi.org/10.1016/j.actamat.2021.116809.

[27] V. Babic, C. Geers, I. Panas, Reactive Element Effects in High-Temperature Alloys Disentangled, Oxidation of Metals 93 (2020) 229–245. https://doi.org/10.1007/s11085-019-09946-6.

[28] V. Babic, C. Geers, B. Jönsson, I. Panas, Fates of Hydrogen During Alumina Growth Below Yttria Nodules in FeCrAl(RE) at Low Partial Pressures of Water, Electrocatalysis 8 (2017) 565–576. https://doi.org/10.1007/s12678-017-0368-8.

[29] A.M. de Andrade, C. Geers, J. Chen, I. Panas, Stress-corrosion cracking sensitization by hydrogen upon oxidation of nickel-base alloys by water – An experiment-guided first-principles study, Journal of Nuclear Materials 595 (2024) 155044. https://doi.org/10.1016/j.jnucmat.2024.155044.

[30] W. Kohn, L.J. Sham, Self-consistent equations including exchange and correlation effects, Phys. Rev. 140 (1965) A1133–A1138.

[31] P. Hohenberg, W. Kohn, Inhomogeneous electron gas, Phys. Rev. 136 (1964) B864–B871.

[32] M.C. Payne, M.P. Teter, D.C. Allan, T.A. Arias, J.D. Joannopoulos, Iterative minimization techniques for ab initio total-energy calculations - molecular-dynamics and conjugate gradients, Rev. Mod. Phys. 64 (1992) 1045–1097.

[33] S.J. Clark, M.D. Segall, C.J. Pickard, P.J. Hasnip, M.I.J. Probert, K. Refson, M.C. Payne, First principles methods using CASTEP, Zeitschrift Fur Kristallographie 220 (2005) 567–570. https://doi.org/10.1524/zkri.220.5.567.65075.

[34] J.P. Perdew, K. Burke, M. Ernzerhof, Generalized gradient approximation made simple, Phys Rev Lett 77 (1996) 3865–3868. https://doi.org/10.1103/PhysRevLett.77.3865.

[35] J.P. Perdew, K. Burke, M. Ernzerhof, Erratum: Generalized gradient approximation made simple (Physical Review Letters (1996) 77 (3865)), Phys Rev Lett 78 (1997) 1396. https://doi.org/10.1103/PhysRevLett.78.1396.

[36] D.R. Hamann, M. Schlüter, C. Chiang, Norm-Conserving Pseudopotentials, Phys Rev Lett 43 (1979) 1494. https://doi.org/10.1103/PhysRevLett.43.1494.

[37] H.J. Monkhorst, J.D. Pack, Special points for Brillouin-zone integrations, Phys. Rev. B 13 (1976) 5188–5192.

[38] J.D. Pack, H.J. Monkhorst, “special points for Brillouin-zone integrations”-a reply, Phys Rev B 16 (1977) 1748–1749. https://doi.org/10.1103/PhysRevB.16.1748.

[39] R.H. Byrd, J. Nocedal, R.B. Schnabel, Representations of quasi-Newton matrices and their use in limited memory methods, Math. Prog. 63 (1994) 129–156.

[40] B.G. Pfrommer, M. Cote, S.G. Louie, M.L. Cohen, Relaxation of crystals with the quasi-Newton method, J. Comput. Phys. 131 (1997) 233–240.

[41] D. Zagorac, H. Müller, S. Ruehl, J. Zagorac, S. Rehme, Recent developments in the Inorganic Crystal Structure Database: theoretical crystal structure data and related features, J Appl Crystallogr 52 (2019) 918–925. https://doi.org/10.1107/S160057671900997X.

[42] S.M. Bruemmer, M.J. Olszta, M.B. Toloczko, D.K. Schreiber, Grain boundary selective oxidation and intergranular stress corrosion crack growth of high-purity nickel binary alloys in high-temperature hydrogenated water, Corros Sci 131 (2018) 310–323. https://doi.org/10.1016/J.CORSCI.2017.11.024.

[43] P.M. Scott, M. Le Calver, Some possible mechanisms of intergranular stress corrosion cracking of Alloy 600 in PWR primary water, in: Proceedings of the Sixth International Symposium on Environmental Degradation of Materials in Nuclear Power Systems - Water Reactors, 1993.

[44] K. Qu, Z. Ding, M. Wu, P. Liu, S. Chen, R. Zhu, B. Han, X. Ma, P. Gao, J. Li, Unraveling atomic-scale lithiation mechanisms in a NiO thin film electrode, J Mater Chem A Mater 8 (2020) 25198–25207. https://doi.org/10.1039/D0TA08415H.

[45] D. Tanguy, Y. Wang, D. Connétable, Stability of vacancy-hydrogen clusters in nickel from first-principles calculations, Acta Mater 78 (2014) 135–143. https://doi.org/10.1016/j.actamat.2014.06.021.

[46] Y. Wang, D. Connétable, D. Tanguy, Hydrogen influence on diffusion in nickel from first-principles calculations, Phys Rev B 91 (2015) 094106. https://doi.org/10.1103/PhysRevB.91.094106.

The Swedish Radiation Safety Authority (SSM) works proactively and preventively with nuclear safety, radiation protection, nuclear security, and nuclear non-proliferation to protect people and the environment from the harmful effects of radiation, now and in the future.

Strålsäkerhetsmyndigheten
SE-171 16 Stockholm
+46 (0) 8-799 40 00
www.stralsakerhetsmyndigheten.se
registrator@ssm.se

Scandinavian Print Group Sweden AB, 2024